Small RNA-sequencing reveals the involvement of microRNA-132 in benzo[a]pyrene-induced toxicity in primary human blood cells

Rima Souki, Jérémy Amosse, Valentine Genet, Morgane Le Gall, Benjamin Saintpierre, Franck Letourneur, Anne Maitre, Christine Demeilliers, Eric Le Ferrec, Dominique Lagadic-Gossmann, et al.

Polycyclic Aromatic Hydrocarbons

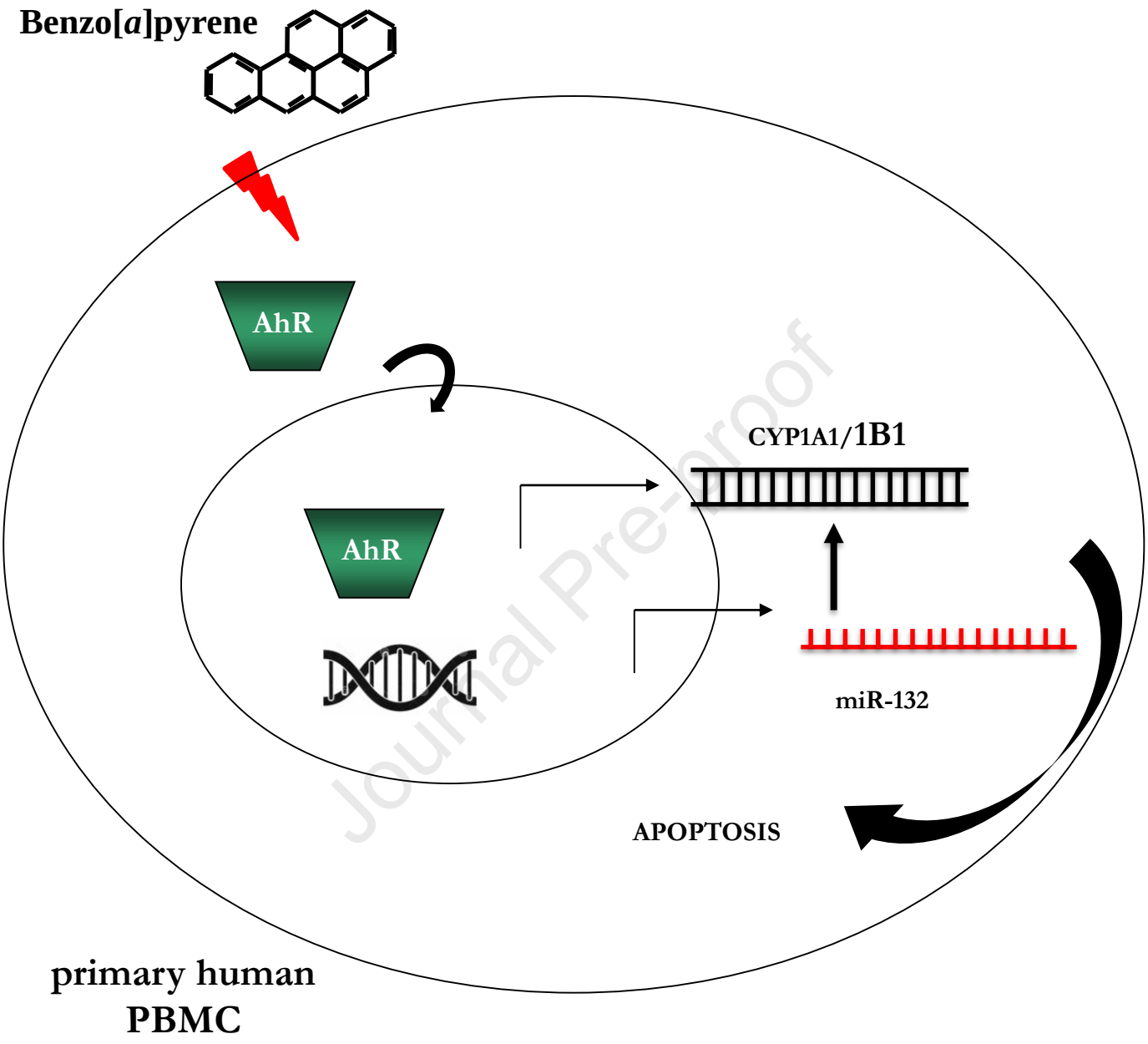

Exposure to polycyclic aromatic hydrocarbons, like benzo[*a*]pyrene, induces miRNA expression changes associated with biological processes relevant to apoptosis in human primary PBMCs.

Small RNA-sequencing reveals the involvement of microRNA-132 in benzo[*a*]pyrene-induced toxicity in primary human blood cells

Rima Souki[1,*], Jérémy Amossé[1,*], Valentine Genêt[1], Morgane Le Gall[2], Benjamin SaintPierre[2], Franck Letourneur[2], Anne Maître[3,4], Christine Demeilliers[3,4], Eric Le Ferrec[1], Dominique Lagadic-Gossmann[1], Normand Podechard[1] and Lydie Sparfel[1]

[1]Univ Rennes, Inserm, EHESP, Irset (Institut de Recherche en Santé, Environnement et Travail), UMR_S 1085, F-35000 Rennes, France

[2] Université Paris Cité, CNRS, INSERM, Institut Cochin, F-75014 Paris, France

[3] Univ. Grenoble Alpes, CNRS, UMR 5525, VetAgro Sup, Grenoble INP, TIMC, EPSP, 38000 Grenoble, France.

[4] Univ. Grenoble Alpes, CHU Grenoble Alpes, Laboratoire de Toxicologie Professionnelle et Environnementale, TIMC, CNRS, Grenoble INP, 38000 Grenoble, France

[*] These authors contributed equally to this work

Corresponding author: Lydie Sparfel, UMR_S 1085, 2 avenue du Pr Léon Bernard, 35043 Rennes, France. Telephone: +33 2 23 23 47 63; Fax: +33 2 23 23 47 94; e-mail: lydie.sparfel@univ-rennes1.fr

Abbreviations: AhR, Aryl Hydrocarbon Receptor; AhRR, AhR Repressor; anti-miR-CTR, miR inhibitor control; anti-miR-132, miR-132 inhibitor; B[*a*]P, benzo[*a*]pyrene ; CYPs, cytochromes P-450; CTP-I, industrial Coal Tar Pitch; CTP-S, synthetic Coal Tar Pitch; DMSO, dimethylsulfoxide; FDR, False Discovery Rate ; IPA, Ingenuity Pathway Analysis; miRNAs, microRNAs; PAHs, Polycyclic Aromatic Hydrocarbons; PBMCs, Peripheral Blood

Mononuclear Cells; PYR, pyrene; RNA-seq, RNA sequencing; TIPARP, TCDD Inducible Poly(ADP-Ribose) Polymerase; UTR, untranslated region; Z-VAD, N-benzyloxycarbonyl-Val-Ala-Asp(O-Me) fluoromethyl ketone

Abstract

Polycyclic aromatic hydrocarbons (PAHs) are widely distributed environmental contaminants, triggering deleterious effects such as carcinogenicity and immunosuppression, and peripheral blood mononuclear cells (PBMCs) are among the main cell types targeted by these pollutants. In the present study, we sought to identify the expression profiles and function of miRNAs, gene regulators involved in major cellular processes recently linked to environmental pollutants, in PBMC-exposed to the prototypical PAH, benzo[*a*]pyrene (B[*a*]P). Using small RNA deep sequencing, we identified several B[*a*]P-responsive miRNAs. Bioinformatics analyses showed that their predicted targets could modulate biological processes relevant to cell death and survival. Further studies of the most highly induced miRNA, miR-132, showed that its up-regulation by B[*a*]P was time- and dose-dependent and required aryl hydrocarbon receptor (AhR) activation. By evaluating the role of miR-132 in B[*a*]P-induced cell death, we propose a mechanism linking B[*a*]P-induced miR-132 expression and cytochromes P-450 (CYPs) 1A1 and 1B1 mRNA levels, which could contribute to the apoptotic response of PBMCs. Altogether, this study increases our understanding of the roles of miRNAs induced by B[*a*]P and provides the basis for further investigations into the mechanisms of gene expression regulation by PAHs.

Keywords: Polycyclic Aromatic Hydrocarbons, Peripheral Blood Mononuclear Cells, microRNAs, Benzo[*a*]pyrene, miR-132-3p, Aryl Hydrocarbon Receptor, Cytochromes P-450 1A1 and 1B1

1. Introduction

Polycyclic aromatic hydrocarbons (PAHs) are a major class of environmental contaminants formed by the incomplete combustion of organic materials, and distillation of coal and petroleum. Human are commonly exposed to these pollutants present in large amounts in food, air pollution, cigarette smoke, and some occupational atmospheres (Mallah et al., 2022). Human exposure to these pollutants has been correlated to various pathologies such as cancer, immunosuppression, and inflammation contributing to cardiovascular and pulmonary diseases (Holme et al., 2019; Stading et al., 2021; Yu et al., 2022). While several particulate PAHs are classified as probable or possible carcinogens by the International Agency for Research on Cancer, benzo[*a*]pyrene (B[*a*]P) is the only PAH classified as a known human carcinogen (International Agency for Research on Cancer, 2010), and the most widely used model compound for studying the effects of PAHs. Most of the B[*a*]P-related toxic effects have been linked to the activation of the aryl hydrocarbon receptor (AhR) and its subsequent binding to specific xenobiotic responsive elements within the promoter of responsive genes such as cytochromes P450 (CYPs) 1A1, 1A2 and 1B1 (Fujii-Kuriyama & Mimura, 2005). We and others showed that activation of the AhR signalling pathway by B[*a*]P produces systemic changes in gene expression contributing in a major way to its toxic effects, especially carcinogenesis in several organs such as lung, liver and lymphoid tissue (Hockley et al., 2006; Sparfel et al., 2010; Liamin et al., 2017, 2018).

MicroRNAs (miRNAs) are short (20 to 23 nucleotides long) non-coding RNAs that regulate gene expression at the post-transcriptional level. Typically, they bind to the 3'-UTR (untranslated region) of target mRNAs, leading to suppression of translation and/or mRNA degradation (Bartel, 2009). Through multiple transcript targets, miRNAs have been shown to regulate many aspects of biology such as stress responses, cell death, or carcinogenesis (Gulyaeva & Kushlinskiy, 2016). More recent investigations have examined the relationship

between environmental contaminants and miRNA expression (Tumolo et al., 2022). Growing evidence linking miRNAs to pollutants, associated with their regulatory role in gene expression, suggests that miRNAs can serve not only as potential biomarkers of exposure but also contribute to the mechanisms of diseases caused by environmental contaminants. Indeed, miRNA alterations after PAH exposure in humans identified patterns that could be responsible for various health outcomes (Deng et al., 2019; Ruiz-Vera et al., 2019).

Peripheral blood mononuclear cells (PBMCs), an easily obtainable blood cell fraction mainly composed of lymphocytes and monocytes, appear to be a major cell type targeted by PAHs. PBMCs are present at the entry points of these contaminants, and circulate permanently through the body, thus acting as the first line of defense. In earlier studies, we have shown that exposure to PAHs inhibits the differentiation of human monocytes into immunocompetent cells such as macrophages (van Grevenynghe et al., 2004). Such an exposure also targets human T lymphocytes, thereby altering their functional properties such as cytokine secretion in current smokers (Prigent et al., 2014) or producing specific B[*a*]P-derived DNA damage associated with an increasing frequency of mutations (Liamin et al., 2017). Overall, these PAH-induced alterations may participate in the immunotoxic, pro-inflammatory or carcinogenic-related effects; this underlines the importance of studying PBMCs to analyse the effect of environmental pollutants to human health. Whether these effects are associated with an alteration of miRNA expression in PBMCs has not been previously investigated. The present study used high-throughput small RNA sequencing (RNA-seq) technology to characterize miRNA changes caused by B[*a*]P exposure in human PBMCs. Using bioinformatics tools, we also investigated the possible role of the differentially expressed miRNAs by predicting their downstream target genes and analysed the major regulated signalling pathways and biological functions. Further analyses showed that B[*a*]P increased, in a dose- and time-dependent manner, the expression of miR-132-3p; that this required AhR activation and that the regulation

104 of CYP1A1/CYP1B1 balance by miR-132 could be a potential modulator of B[*a*]P's
105 cytotoxicity in PBMCs.
106

2. Materials and methods

2.1. Chemicals and reagents

B[*a*]P, pyrene (PYR), dimethylsulfoxide (DMSO), Hoechst 33342, CH-223191, and N-benzyloxycarbonyl-Val-Ala-Asp(O-Me) fluoromethyl ketone (Z-VAD) were obtained from Merck (Darmstadt, Germany). Lipofectamine and SYTOX®Green were purchased from Thermo Fisher Scientific (Courtaboeuf, France). PAH complex mixtures were extracted from the industrial products coal tar pitch (CTP-I), and the synthetic coal tar pitch mixture (CTP-S) was identically reconstituted using PAH standards as previously reported (Bourgart et al., 2019); PAH profiles in CTP-I are indicated in Supplementary materials and methods (Table S1). The applied dose was adjusted to 10 nM and 2 µM of B[*a*]P for CTP-I and CTP-S.

2.2. Cell culture and treatment

PBMCs were isolated from buffy coats collected from human blood donor who provided written informed consent for the research protocol according to the regulation for blood transfusion of the French blood organization Etablissement Français du Sang, Rennes (France), AC-2019-3853 by Ficoll (Eurobio, Les Ulis, France) gradient centrifugation (Liamin et al., 2017, 2018). They were then cultivated at 37°C with 5% CO2 in RPMI medium (Eurobio) supplemented with 20 IU/mL penicillin, 20 µg/mL streptomycin, and 10% decomplemented fetal calf serum (Lonza, Bale, Swiss) and exposed to PAHs, stocked in DMSO. The final concentration of DMSO in the culture medium was always < 0.2% v/v and control cultures received the same dose of DMSO as treated cultures.

2.3. RNA isolation

Parallel isolation of small and large RNA from PBMCs was perfomed using the NucleoSpin RNAs kit (Macherey-Nagel, Düren, Germany) with minor changes, and were quantified as detailed in Supplementary materials and methods.

2.4. RT-qPCR assays

The reaction is performed on total RNA (1 µg),reverse-transcribed into cDNA using the RT Applied Biosystems kit (Thermo Fischer Scientific). For qPCR assays,gene-specific primers from Eurogentec (Seraing, Belgium) were used as previously described (Liamin et al., 2018).

The small RNA fraction (5 ng) was reverse-transcribed using an adapter-based TaqMan Advanced miRNA cDNA Synthesis kit (Thermo Fischer Scientific) with a preamplification step according to the manufacturer's protocol. For qPCR assays, predesigned probe-based TaqMan Advanced miRNA Assays and TaqMan Fast Advanced Master Mix (Thermo Fisher Scientific) were used. For qPCR validation, we spiked the samples with an exogenous miRNA (miR-39) for normalization before RNA extraction, and used it as the reference miRNA to control technical variability as recommended (Hu et al., 2020).

2.5. Western blotting

Total cellular protein extracts were prepared by lysis of PBMCs in a buffer containing 50 mM Tris-HCl, pH 8, 5 mM EDTA, 150 mM NaCl, 1% Nonidet-40, 0.5% sodium desoxycholate, 1 mM sodium fluoride, 2 mM dithiothreitol, 1 mM sodium orthovanadate and 1 mM phenylmethanesulphonyl fluoride, supplemented with a cocktail protease inhibitor (Roche Diagnostics, Meylan, France).

Protein separation was performed on a polyacrylamide gel followed by electrophoresis transfer onto nitrocellulose membranes (Merck Millipore, Burlington, MA, USA). After blocking, membranes were incubated with a mouse monoclonal antibody to human Dicer (ab14601) (Abcam, Cambridge, UK) or with a rabbit anti-human PUMA antibody (Cell Signaling Technology, Danvers, MA, United States). A peroxidase-conjugated antibody was next used as secondary antibody and immunolabelled proteins were visualized by chemoluminescence using a gel imaging system (Bio-Rad) equipped with a CCD camera. Protein amounts were quantified by densitometry using Image Lab™ software (Bio-Rad) and

normalized using HSC70 (Santa Cruz Biotechnology (Heidelberg, Germany) as a loading control.

2.6. Small RNA-seq

2.6.1. Library preparation and small RNA-seq

To construct the libraries, 12 independent PBMC cultures each grown in untreated (DMSO) and 2 µM B[*a*]P-treated conditions for 48 h, were combined in 3 equal pools (with 4 separate blood donors *per* pool) for each condition. Due to the biological variability between donors (Sparfel et al., 2010; Liamin et al., 2018), we pooled the 12 cultures in 3 equal pools, either with or without B[*a*]P exposure, prior to isolate 5-15 ng of the small RNA fraction and processed using Qiaseq miRNA library prep kit (Qiagen, Hilden, Germany) according to the manufacturer's instructions and as detailed in Supplementary materials and methods. Sequences obtained in the study have been deposited in GenBank with accession numbers GSE222837. After filtering low-quality reads and adaptor sequences, a total of 3251955 $\pm$ 468873 and 2604815 $\pm$ 227816 miRNA reads were obtained for the untreated (DMSO) and B[*a*]P-treated PBMCs, respectively (Tables S3 and S4).

2.6.2. Small RNA-seq data processing and mapping

Fastq files were aligned using the QIAGEN pipeline (QIAseq® miRNA Primary Quantification). The number of differentially expressed miRNAs between the two conditions were determined with the DESeq2 R package (DESeq2_1.26.0). The standard DESeq2 normalization method (DESeq2's median of ratios with the DESeq function) was used, with a pre-filter of reads and genes (reads uniquely mapped on the genome, or up to 10 different loci with a count adjustment, and genes with at least 10 reads in at least 3 different samples). Following the package recommendations, the Wald test was used with the contrast function and the Benjamini-Hochberg False Discovery Rate (FDR) control procedure to identify differentially expressed genes.

2.7. Functional analysis

Lists of miRNAs significantly induced or repressed after B[*a*]P exposure were analysed through the use of Ingenuity Pathway Analysis (IPA) software (QIAGEN Inc., https://www.qiagenbioinformatics.com/products/ingenuity-pathway-analysis v. 73620684). Significantly over-represented functions were identified with a right-tailed Fisher's Exact Test that calculates an overlap *p-value* determining the probability that each term associated with our list of differential miRNAs was due to chance alone.

2.8. miRNA transfection

To study the functions of miR-132, PBMCs were transfected with 8.5 x 10^{-9} M miR-132 inhibitor (anti-miR-132) or miR inhibitor control (anti-miR-CTR) (Thermo Fisher Scientific) using lipofectamine. Twelve hours later, PBMCs were exposed to 2 µM B[*a*]P for 48 h.

2.9. Cell death evaluation

PBMCs were tested for both apoptotic and necrotic cell death, as previously reported (van Meteren et al., 2019). Apoptotic cells were identified by chromatin condensation and morphological changes of the nucleus using the blue-fluorescence chromatin dye Hoechst 33342; in parallel, necrotic cells were evidenced by the SYTOX®Green nucleic acid stain, only permeant to cells with compromised plasma membranes. Briefly, untreated (DMSO) and PAH-treated PBMCs were stained at 37 °C with 10 µg/ml Hoechst 33342 and 125 µM SYTOX®Green for 15 minutes. Apoptotic and necrotic cells were then manually counted using a fluorescence microscope (Axio Scope A1, ZEISS, Marly le Roi, France); a total of 300 nuclei were examined for each condition (magnification x40).

2.10. Statistical analysis

Data are expressed as mean ± SEM from at least 3 independent experiments. Statistical significance was assessed using GraphPad Instat (GraphPad Software, INC., La Jolla, CA,

205 USA) by paired Student's t-test, or analysis of variance followed by Dunnett or Student-
206 Newman-Keuls post hoc tests. A *p-value* ≤ 0.05 was considered significant.
207

3. Results

3.1. Identification of B[*a*]P-regulated miRNAs in human PBMCs using high throughput small RNA-seq

We isolated primary human PBMCs from healthy blood donors and treated them with vehicle (DMSO) or with the prototypical PAH, B[*a*]P, at previously and commonly chosen concentrations for *in vitro* toxicity studies of 10 nM and 2 µM (Liamin et al., 2017) for 48 h. The expression of four well-known AhR-target genes (*CYP1A1*, *CYP1B1*, AhR Repressor (*AhRR*), and TCDD Inducible Poly(ADP-Ribose) Polymerase (*TIPARP*)) was analysed in PBMCs by RT-qPCR. As expected (Hockley et al., 2006; Sparfel et al., 2010), a 48-h exposure to 2 µM B[*a*]P was found to up-regulate the mRNA expression of these AhR-target genes, with statistically significant induction of *CYP1A1* and *CYP1B1* while no significant difference was observed in PBMCs treated with 10 nM B[*a*]P (Figure 1A). We then investigated the effect of 2 µM B[*a*]P on the expression of genes and proteins involved in the miRNA processing machinery. As shown in Figure 1B, *DROSHA*, *DCRG8*, *XPO5*, *DICER* and *AGO2* mRNA expression was not affected. Consistent with the unaltered mRNA levels, protein levels for DICER were not significantly increased in the presence of B[*a*]P (Figure 1C). Taken together, these data indicate that primary human PBMCs fully responded to a 2 µM B[*a*]P 48 h exposure, and possess components of the miRNA machinery unaltered by such exposure, allowing an analysis of global changes in miRNA profiles in these conditions.

To identify differentially expressed miRNAs in response to B[*a*]P exposure, we performed deep sequencing of small RNAs extracted from PBMCs from 12 independent donors cultured in the presence of 2 µM B[*a*]P or DMSO for 48 h. As shown in Figure 2A, B[*a*]P treatment did not significantly alter the proportion of miRNA reads which accounted for approximately 28% and 25% of the total number of reads for DMSO and B[*a*]P-treated samples, respectively. Overall, we detected 765 mature known miRNAs expressed with a base mean of reads > 10 in at least

one of the two conditions (Table S5), with 436 (57%) shared by the two conditions as shown by the Venn diagram (Bardou et al., 2014) (Figure 2B). By using the principal component analysis on the top 500 miRNA reads, we revealed distinct clusters between untreated (DMSO) and B[*a*]P-treated PBMCs (Figure S1). After filtering with an adjusted *p-value* $\leq$ 0.05 and a |log2FoldChange| $\geq$ 0.4 or $\leq$ -0.4, 285 miRNAs showed differential expression after B[*a*]P treatment compared with the DMSO control with 65 up-regulated and 220 down-regulated miRNAs (Figure 2C, Table S6). Using as a cutoff miRNAs with more than $\geq$ 100 read counts in at least one of the 6 conditions, 15 miRNAs whose expression was altered upon B[*a*]P treatment were detected, including 4 up-regulated miRNAs (miR-132-3p, miR-1246, miR-3069, and miR-320c) and 11 down-regulated miRNAs (miR-221-3p, miR-23b-3p, mir-454-3p, miR-7-5p, miR-30c-5p, miR-142-3p, miR-144-5p, miR-301a-3p, miR-4515, miR-1909-5p, miR-6815-5p) (Figure 2E). The heatmap (Figure 2D) indicated that these differentially-regulated miRNAs were well clustered into 2 classes defining distinct expression patterns between untreated (DMSO) and B[*a*]P-treated PBMCs.

3.2. Functional analysis and target gene prediction of B[*a*]P-regulated miRNAs in human PBMCs

To explore the over-represented functions in which these 15 B[*a*]P-regulated miRNAs are involved, we used IPA software. Cellular development, growth/proliferation and death/survival-related functions were 3 of the top 5 functions altered in response to B[*a*]P treatment (Table 1). The use of the TAM 2.0 tool to perform functional annotations of B[*a*]P-regulated miRNAs by over-representation analysis also reported an enrichment in miRNAs contributing to cell death and apoptosis (Table S7).

Since the functional enrichment analysis of miRNAs is limited by current miRNA functional annotations, we performed a target gene prediction of the 15 differentially-regulated

miRNAs using the four analysis online tools, TargetScan, FunRich, miRDIP, and miRWALK. We thus identified 313 common genes (Figure S2A). IPA software was then used to analyse the most significant diseases and disordered biological functions linked to these genes. As shown in Table S8, the most significant disease was cancer, the most significant molecular and cellular function was linked to function and maintenance, and organismal survival appeared as the most significant category in physiological development and system function. Using the online prediction tool WebGestalt, we then performed an identification of enriched categories based on a FDR $\leq$ 0.05 for the 313 predicted target genes. Interestingly, the GO biological process analysis showed that these genes are involved in the negative regulation of intrinsic apoptotic signalling pathway to DNA damage, and in the regulation of cellular senescence (Figure S2B). The KEGG analysis also identified autophagy among the five most significant categories selected on *p-value* (Figure S2C). Altogether, these results indicate that the differentially-regulated miRNAs and their predicted genes may participate in regulation of the balance between cell survival and death.

3.3. Validation of B[*a*]P-regulated miRNAs and associated biological pathways in human PBMCs by RT-qPCR

We then performed RT-qPCR assays using cultures of independent PBMC samples, in order to confirm the transcriptional changes of miRNAs identified by the RNA-seq analysis. From the list of the 15 most differentially-regulated miRNAs, we selected 8 miRNAs (miR-132-3p, miR-1246, miR-3609, miR-221-3p, miR-454-3p, miR-7-5p, miR-30c-5p, miR-142-3p) that demonstrated the highest reads and depending on TaqMan probes available for RT-qPCR validation. As shown in Figure 3A, all the miRNAs examined show a trend consistent with the miRNA-seq results. We detected levels of up-regulation for miR-132, miR-1246, miR-3609 and lower levels for miR-221, miR-454, miR-7, miR-30c, miR-142 in B[*a*]P-treated PBMCs

(Figure 3A). However, results of RNA-seq data were more pronounced than those obtained by RT-qPCR results; indeed, regarding these latter results, the effect of B[*a*]P was only statistically significant for miR-132 (Figure 3A). Due to its highest change in expression and the robustness of its analysis, miR-132 was selected for further investigations. To further evaluate the impact of B[*a*]P on miR-132 expression, PBMCs were exposed to B[*a*]P at increasing concentrations and times. We showed that miR-132 increased with B[*a*]P concentration with a significant effect from 2 µM compared to DMSO-controls (Figure 3B). Time-course of its induction in PBMCs exposed to 2 µM B[*a*]P showed that miR-132-3p miRNA levels increased over time and became significantly up-regulated at 48 h (Figure 3C).

Due to the ontology analysis, and since B[*a*]P is known to initiate cell death in different cell types (Hardonnière et al., 2017), we evaluated whether B[*a*]P caused apoptosis, necrosis, and/or autophagy in PBMCs. Using Hoechst 33342 and SYTOX®Green co-staining, we first observed that the number of apoptotic PBMCs increased with B[*a*]P concentrations and was significant at 2 µM B[*a*]P after a 48 h-exposure (Figure 4A) with several apoptotic morphological features such as chromatin condensation and DNA fragmentation (magnified images on theright panel, Figure 4A). By contrast, B[*a*]P treatment did not cause any significant changes in the number of necrotic cells (Figure 4A). Additionally, analysis by RT-qPCR experiments revealed that the expression of several genes involved in the regulation of the apoptotic signalling pathway in response to DNA damage by p53 were increased after treatment with 2 µM B[*a*]P for 48 h (Figure 4B). A significant increase was notably found for *DDB2*, which plays a central role in defining the response to DNA damage as well as for the pro-apoptotic genes *BBC3* and *BID* (Figure 4B). In agreement with mRNA expression, protein levels of PUMA encoded by the *BBC3* gene were also significantly increased after treatment with 2 µM B[*a*]P for 48 h (Figure 4C). Next, we examined cell autophagy by acridine orange staining and flow cytometry to assess acidic vacuoles, that increase upon autophagy induction

(Thomé et al., 2016). We found that the percentage of acridine orange-stained cells was not significantly altered upon B[*a*]P treatment (Figures S3A and S3B). Furthermore, treatment with 2 µM B[*a*]P for 48 h did not significantly alter mRNA levels of typical markers of autophagy such as *ATG5*, *ATG7*, *ATG12*, and *BECLIN1* (Figure S3C) or the protein LC3 conversion (LC3B-I to LC3B-II) (Figure S3D) (Mizushima & Yoshimori, 2007). Finally, given the association of oxidative stress with cell death/survival, we used the oxidative-sensitive H2DCFDA probe and flow cytometry to detect generation of reactive oxygen species in PBMCs exposed to B[*a*]P for 48 h. As shown in Figure S4A, a 48-h treatment with 10 nM or 2 µM B[*a*]P did not modify the production of reactive oxygen species. However, we observed alterations in the expression of markers linked with the oxidative machinery; we thus found a significantly decreased mRNA expression of *SOD2* mRNA and *HMOX1*/HO-1 mRNA and protein levels after B[*a*]P treatment with 2 µM for 48 h (Figures S4B and S4C), therefore suggesting that an early oxidative stress probably could contributes to B[*a*]P-induced apoptosis as previously described (Huc et al., 2007).

3.4. Role of miR-132 in B[*a*]P-induced cell death in human PBMCs

In the next set of experiments, we first investigated the involvement of the apoptosis induced by B[*a*]P in miR-132 expression using Z-VAD, an apoptosis inhibitor (Fearnhead et al., 1995; van Meteren et al., 2019). Although Z-VAD prevented the increase in the number of apoptotic cells (Figure 5A, right panel), it did not change the B[*a*]P-induced miR-132 expression (Figure 5A), thus indicating that this was not mediated by apoptosis. We next examined the effects of the potent AhR antagonist CH-223191 (Zhao et al., 2010), inhibiting B[*a*]P-induced CYP1A1 and CYP1B1 mRNA levels in PBMCs (data not shown) on the miR-132 up-regulation. Interestingly, CH-223191 strongly inhibited miR-132-induced expression in B[*a*]P-treated PBMCs (Figure 5B); it also significantly prevented the induction of apoptosis in B[*a*]P-treated

PBMCs (Figure 5B, right panel). We thereafter analysed the effects of several AhR activators on miR-132. PYR, known as a weak activator of AhR (Boonen et al., 2020), failed to increase miR-132 levels (Figure 5C). By contrast, realistic and synthetic CTPs, adjusted at concentrations of 10 nM and 2 µM B[*a*]P and containing 17.3 nM and 3.46 µM PYR respectively, markedly increased miR-132 expression in PBMCs (Figure 5D). Interestingly, PYR, did not significantly induce apoptosis whereas real and synthetic PAH mixtures significantly increased apoptotic PBMCs (Figures 5C and 5D, right panels). Altogether, these data indicate that B[*a*]P-induced AhR activation is necessary to increase miR-132 levels and cause apoptosis in PBMCs at a 48 h-exposure.

We further analysed the role of miR-132 on B[*a*]P-induced effects in human PBMCs. Firstly, we explored the effects of miR-132 knockdown on B[*a*]P-induced apoptosis by transfecting PBMCs with an anti-miR-132 or with an anti-miR-CTR. Transfection and knockdown efficiencies were confirmed by measuring miR-132 expression levels in PBMCs (Figure S5A). The results showed that transfection of the anti-miR-132 significantly mitigated the number of B[*a*]P-induced apoptotic PBMCs compared to PBMCs transfected with the anti-miR-CTR (Figure 6A). Interestingly, RT-qPCR analysis showed that transfection with the anti-miR-132 in B[*a*]P-treated PBMCs did not alter the mRNA expression of pro-apoptotic and anti-oxidative genes such as *BBC3* and *Bcl2* (Figure 6B) and of *SOD2* and *HMOX1*, respectively(Figure S5B). Since we observed a strong decrease in expression of AhR target genes, *CYP1A1* and *CYP1B1* associated with the increased miR-132 expression over 48 h (Figure 6C), we explored a potential regulatory role for miR-132 in the AhR signalling pathway and activation of its downstream genes. Interestingly, transfection with the anti-miR-132 increased B[*a*]P-induced, although not significantly, *CYP1A1* mRNA levels, and significantly decreased those of *CYP1B1* (Figure 6D), while it did not modify *AhR* or *ARNT* expression when compared to B[*a*]P-treated PBMCs transfected with the anti-miR-CTR (Figure 6E). Altogether,

358 these data suggest an effect of B[*a*]P on the CYP1A1/CYP1B1 balance, which could be
359 associated with its induction of apoptosis in PBMCs.
360

Discussion

miRNAs play major roles in the regulation of responses to environmental stresses and pollutant exposures. Alteration of their expression can influence a variety of cellular functions, which justifies investigating their expression profiles to understand toxicological responses of various cell types. Among ubiquitous pollutants, PAHs, especially the prototypical B[*a*]P, exert various toxic effects, mainly associated with AhR activation and the subsequent induction of CYP1-metabolizing enzymes (Shimada, 2006). We have previously characterized B[*a*]P-induced alterations and their involvement in immunotoxic, pro-inflammatory or carcinogenic effects using primary human blood cells (Liamin et al., 2017; Prigent et al., 2014; van Grevenynghe et al., 2004). However, the key questions of how miRNA expression is regulated and what the roles of dysregulated miRNAs are in B[*a*]P-exposed human blood cells, remain to be elucidated. In the present study, primary human PBMCs representing normal non-transformed human cells that express all the miRNA processing machinery (Beer et al., 2014), were used as a model system to assess the effect of B[*a*]P on the expression of miRNAs.

Recent advances in next-generation sequencing technologies have enabled the development of comprehensive and robust approaches such as small RNA-seq to quantify miRNA expression genome-wide. To our knowledge, this is the first study using the high-throughput small RNA-seq method to profile B[*a*]P-regulated miRNAs, which allowed us to identify them as potential novel modulators of the effects of B[*a*]P, on human PBMCs. We observed that B[*a*]P altered the expression of 285 miRNAs, most of them being down-regulated. This down-regulation has previously been described, notably the effects of PAHs and cigarette smoke on miRNA profiles in humans have been reported (De Flora et al., 2012; Deng et al., 2014). By selecting highly expressed miRNAs, we focused on 15 miRNAs whose expression is altered in B[*a*]P-treated PBMCs. Some of these miRNAs have already been associated with B[*a*]P treatment such as miR-221 (recently proposed as a genetic marker for

bladder cancer for which PAH exposure is a risk factor; Martin-Way et al., 2022), miR-30c regulated by B[*a*]P exposure (Wu et al., 2019) or miR-142, a PAH-responsive marker in epidemiological studies (Rani, 2021). In the context of realistic environmental exposure to which a human may be exposed, a number of such miRNA signatures have been described, for example, miR--30c and miR-142 for cigarette smoke, and the miR-144 for air pollution by diesel particles (Vrijens et al., 2015). The miR-132 also appeared regulated under human exposure to cigarette smoke (Donate et al., 2021), our use of an occupational mixture of coal tar reinforces this data in a real exposure situation. Interestingly, our *in silico* analysis indicated that these 15 differentially-expressed miRNAs and their predicted targets could be enriched in link with various functions, including well-documented B[*a*]P-regulated processes and signalling pathways. Indeed, IPA analysis revealed the prominence of biological categories involved in apoptosis and autophagy processes essential to cell death and survival, which we have previously been reported to be associated with B[*a*]P exposure (Lagadic-Gossmann et al., 2019). Analysis of signalling pathways activated by B[*a*]P-regulated miRNAs and their targets genes such as *MDM2* and *DDB2* support involvement of PI3K-Akt pathway and DNA damage response. DNA damage-induced Akt activation provides an opportunity for cells to survive and repair DNA damage as we reported (Liamin et al., 2017). The consequence of DNA damage depends on the balance between death and survival signals even if the molecular basis underlying the balance between death and survival remains to be clarified under such our experimental conditions. Our experimental data confirmed that exposure of PBMCs to B[*a*]P induces cell apoptosis, supporting the hypothesis that miRNAs altered by B[*a*]P might be implicated in the cellular alterations caused by this pollutant in PBMCs. Subtle regulation of miRNAs has been described as able to significantly inhibit different individual key targets to modify biological responses (Flynt & Lai, 2008). For example, miR-221, known to promote cell growth and protect cell from apoptosis (Liu et al., 2020; Xie et al., 2018), appeared weakly

down-regulated in B[*a*]P-treated PBMCs whereas its pro-apoptotic target *BBC3*/PUMA was up-regulated at both mRNA and protein levels. A down-regulation of miR-142, leading to changes in gene expression associated with an increase in B[*a*]P-DNA adducts in lung and liver tissues, has also been reported (Halappanavar et al., 2011).

In the present study, we focused on miR-132 as it was the only miRNA whose altered expression was validated by RT-qPCR. When we used TaqMan advanced probe-based technology to validate miRNAs on independent PBMC samples, we did not statistically validate by RT-qPCR the changes in expression of the 15 miRNAs identified by RNA-seq. Although the consistency of these two techniques has been described (Yagi et al., 2017), discrepancies have also been reported leading to a low percentage of validation by RT-qPCR (Chettimada et al., 2020; Ogando et al., 2016). This could be due not only to a difference in the specificity between targeted qPCR *versus* whole library amplification of RNA-seq, but also to a difference in the approaches used for data normalization. Indeed, non-variable small RNAs have not been proposed for normalization in qPCR as there is no standard strategy (Prieto-Fernández et al., 2019). Nevertheless, the trends in the qPCR quantification of selected miRNAs was consistent with the RNA-seq results, supporting the validity of the sequencing data.

Interestingly, the most induced miRNA, the miR-132, is a highly conserved miRNA belonging to the cluster miR212/132 associated with pleiotropic roles in multiple cell types and different biological processes such as neurological development, inflammation, angiogenesis and cancer (Wanet et al., 2012). miR-132 has also been described as regulated in several immune contexts such as experimental autoimmune encephalomyelitis (Hanieh & Alzahrani, 2013), in patients suffering from arthritis (Donate et al., 2021) or multiple sclerosis (Sağır et al., 2021). Regarding its transcriptional regulation, miR-132 appears typically controlled by the cAMP-response element binding transcription factor (Wanet et al., 2012), but in inflammatory

contexts, recent evidences demonstrated that AhR activation is implicated in the regulation of miR-132 expression (Hanieh & Alzahrani, 2013; Abdullah et al., 2019; Donate et al., 2021). Our data demonstrated the major contribution of AhR in B[*a*]P-induced miR-132 expression in PBMCs. Indeed, realistic and synthetic CTPs with B[*a*]P content enhanced miR-132 expression, whereas the weak AhR agonist PYR exhibiting low AhR activity (Boonen et al., 2020) did not significantly alter miR-132 levels. In addition, the AhR antagonist CH-223191 fully counteracted the induction of miR-132 expression by B[*a*]P, whereas the use of pifthrin-α, a p53 inhibitor, also reducing B[*a*]P metabolism (Sparfel et al., 2006), did not change it (data not shown). Our findings are consistent with the description of an AhR binding consensus motif located in the miR-132 gene, as described by Hanieh et al., (2015). Despite these advances indicating the involvement of AhR in the B[*a*]P-induced miR-132 expression independently from metabolism and activation of p53 pathway, the transcriptional control of the miR-132 expression by AhR remains incompletely elucidated. Although the induction of miR-132 by AhR has been suggested to play an important role in mediating some of the immunomodulatory effects of AhR (Wanet et al., 2012), its exact role in PBMCs awaits further investigation. Since PYR did not induce up-regulation of miR-132 in PBMCs and because CH-223191 concomitantly decreased B[*a*]P-triggered apoptosis and miR-132 up-regulation, we first postulated a role of miR-132 in apoptosis. To ascertain this role, B[*a*]P-induced miR-132 expression was inhibited *via* an anti-miR-132 that mitigated apoptosis in B[*a*]P-treated PBMCs, in agreement with the proposed role of miR-132 as a tumor suppressor in mantle cell lymphoma (B. Wu et al., 2020). By antagonizing miR-132 in PBMCs, the mRNA expression levels of pro- and anti-apoptotic genes remained unchanged while those of CYP1A1 and CYP1B1 were altered. Then, we hypothetized that miR-132 might modulate the CYP1A1/CYP1B1 balance. Since CYP1A1 is important for detoxication whereas CYP1B1 plays a prominent role in the metabolic activation and genotoxicity of PAHs (Uno et al., 2006), we propose that modulation

by miR-132 in favour of CYP1B1 could be correlated to B[*a*]P-induced apoptosis. However, the mechanism by which B[*a*]P-induced miR-132 regulates CYP1A1 and CYP1B1 mRNAs remains to be determined. Interestingly, a negative correlation between miR-132 and CYP1A1 has already been described (Rieger et al., 2013). Moreover, the description of miR-132 binding sites on the CYP1A1 3'UTR in the miRWALK database suggests a direct regulation of CYP1A1 by miR-132 through transcript degradation. To our knowledge, no studies have so far linked miR-132 to CYP1B1 but an indirect transcriptional regulation mediated by a down-regulation of the SIRT1 deacetylase that regulates CYP is possible (Lee et al., 2010). A role for cAMP also cannot be ruled out since we have previously reported that the B[*a*]P-activated β2-adrenoreceptor-depending signalling pathway is crucial for PAH-mediated up-regulation of CYP1B1 (Lagos et al., 2010; Mayati et al., 2012). We then propose a model in which B[*a*]P-induced miR-132 mediates an increase of CYP1B1, associated to a reduction of CYP1A1 mRNA levels, thus potentiating the apoptotic response of PBMCs. Biological functions mediated by these potential miR-132 targets are worthy of further investigations in the future, especially during exposure to xenobiotics.

Conclusion

Our results contribute to a better understanding of the roles of miRNA, particularly that of miR-132, in the response to B[*a*]P exposure in human PBMCs, and provide the foundations for further investigations on the regulatory mechanisms of gene expression associated with PAH exposure.

Acknowledgments

This work was supported by The French National Research Program for Environmental and Occupational Health of Anses (2019/1/010). Rima Souki had a doctoral fellowship from the

French Ministry for Higher Education and Research and Jeremy Amosse was a post-doctoral recipient from Anses. We are also thankful to the faculty of Pharmacy of Rennes, for funding the extended contract of Rima Souki. We thank Dr Catherine Lavau for critical reading of the manuscript and English editing. The authors are also grateful to the flow cytometry platform of Biosit, University of Rennes 1 (France).

Legends of figures

Fig.1: Primary human PBMCs are fully responsive to 2 µM B[*a*]P exposure for 48 h and express several components of the miRNA machinery. Primary human PBMCs were treated with vehicle (DMSO), with 10 nM or 2 µM B[*a*]P for 48 h. (A, B) mRNA expression of AhR-target genes (A) and miRNA machinery genes (B) was measured by RT-qPCR. Data are expressed relative to mRNA expression levels in DMSO-treated PBMCs, arbitrarily set at 1 unit and are shown as mean ± SEM of 8 (A) and 4 (B) independent experiments performed with PBMCs from separate blood donors tested in triplicate *per* experiment. (C) Expression of DICER protein was analyzed by Western blotting. HSC70 was used as a loading control. A representative blot is displayed on the right panel. Data are expressed relative to protein expression levels in DMSO-treated PBMCs, arbitrarily set at 1 unit and are shown as mean ± SEM of 5 independent experiments performed with PBMCs from separate blood donors. *, $p \leq 0.05$ when compared with DMSO-treated PBMCs (analysis of variance followed by Dunnett's multirange test) (A).

Fig.2: Identification of B[*a*]P-regulated miRNAs in human PBMCs using high-throughput small RNA-seq. Primary human PBMCs were treated with vehicle (DMSO) or 2 µM B[*a*]P for 48 h and small RNA-seq was used to profile miRNA expression. (A) Distribution of percentages of differentially mapped miRNAs. (B) Venn diagram showing numbers of shared and unique miRNAs expressed in PBMCs. miRNAs were identified with a base mean of reads > 10 in at least one of the two conditions. (C) Volcano plot of the differentially expressed miRNAs with log2(Fold Change) on the x-axis and -log10(adjusted *p-value*) on the y-axis. Genes with an adjusted *p-value* ≤ 0.05 and a log2(Fold Change) ≥ 0.4 or ≤ -0.4 are highlighted in bright red for the up-regulated annotations, representing a total of 65 miRNAs, and bright blue for down-regulated annotations, with a total of 220 miRNAs. (D) Visual heatmap representation of the top 15 miRNAs (http://www.heatmapper.ca/expression) showing

unsupervised hierarchical clustering performed on rows (miRNAs) and columns (samples) using Spearman rank correlation on z-scored normalized counts. (E) Table indicating differential expression of the top highest expressed 15 miRNAs significantly regulated after B[*a*]P exposure.

Fig.3: Selected B[*a*]P-regulated miRNAs identified by RNA-seq are validated by RT-qPCR in human PBMCs. Primary human PBMCs were treated with vehicle (DMSO) or 2 µM B[*a*]P for 48 h (A), with various increasing B[*a*]P concentrations for 48 h (B) or with 2 µM B[*a*]P for various increasing times (C). miRNA expression was measured by RT-qPCR. Data are expressed relative to miRNA expression levels in DMSO-treated PBMCs (dotted black line), arbitrarily set at 1 unit and are shown as mean ± SEM of 12 (A), 5 (B) and 6 (C) independent experiments performed with PBMCs from separate blood donors tested in triplicate *per* experiment. *, $p \leq 0.05$ when compared with DMSO-treated PBMCs (paired Student's *t* test (A) and analysis of variance followed by Dunnett's multirange test (B, C)).

Fig.4: B[*a*]P induces apoptosis in human PBMCs. Primary human PBMCs were treated with vehicle (DMSO), with 10 nM (A) or 2 µM B[*a*]P (A, B, C) for 48 h. (A) Apoptosis was identified by microscopic observation (magnification x40) of the number of cells with condensed and/or fragmented chromatin after nuclear staining by Hoechst 33342, and necrosis was estimated by SYTOX®Green staining. Representative photographs are displayed on the right panel with digitally magnified images (x5) indicating apoptotic features such as chromatin condensation and DNA fragmentation. Data are expressed as percentages of dead cells and are shown as mean ± SEM of 5 independent experiments performed with PBMCs from separate blood donors. (B) mRNA expression of genes involved in DNA damage and apoptosis was measured by RT-qPCR. Data are expressed relative to mRNA expression levels in DMSO-

543 treated PBMCs, arbitrarily set at 1 unit and are shown as mean ± SEM of 8 independent
544 experiments performed with PBMCs from separate blood donors tested in triplicate *per*
545 experiment. (C) Expression of PUMA protein was analyzed by Western blotting. HSC70 was
546 used as a loading control. A representative blot is displayed on the right panel. Data are
547 expressed relative to protein expression levels in DMSO-treated PBMCs, arbitrarily set at 1
548 unit and are shown as mean ± SEM of 6 independent experiments performed with PBMCs from
549 separate blood donors. *, $p \leq 0.05$ when compared with DMSO-treated PBMCs (analysis of
550 variance followed by Dunnett's multirange test (A) and paired Student's *t* test (B, C)).
551
552 **Fig.5: B[*a*]P-induced miR-132 expression does not depend on apoptosis but on AhR**
553 **activation in human PBMCs.** miR-132 expression was measured by RT-qPCR in primary
554 human PBMCs pre-treated or not for 1 h with 10 µM Z-VAD (A) or with 3 µM CH-223191
555 (B) prior to a B[*a*]P treatment for 48 h (A, B), with the vehicle (DMSO) or 2 µM PYR for 48 h
556 (C) or with industrial and synthetic CTP mixtures (CTP-I and CTP-S) (D). (A, B, C, D, left
557 panels) miR-132 expression was measured by RT-qPCR. Data are expressed relative to miRNA
558 expression levels in DMSO-treated PBMCs, arbitrarily set at 1 unit and are shown as mean ±
559 SEM of 6 (A, B), 8 (C), 7 (D, CTP-I) and 6 (D, CTP-S) independent experiments performed
560 with PBMCs from separate blood donors tested in triplicate *per* experiment. (A, B, C, D, right
561 panels) Apoptosis was identified by microscopic observation of the number of cells with
562 condensed and/or fragmented chromatin after nuclear staining by Hoechst 33342 staining. Data
563 are expressed as percentages of dead cells and are shown as mean ± SEM of 4 (A), 5 (B), 8 (C)
564 and 6 (D) independent experiments performed with PBMCs from separate blood donors. *, $p \leq$
565 0.05 when compared with B[*a*]P (A, B)- and DMSO (D)-treated PBMCs (analysis of variance
566 followed by the Student-Newman-Keuls's multirange test (A, B) or by Dunnett's multirange
567 test (D)).

Fig.6: miR-132 inhibition regulates B[*a*]P-induced CYP1A1 and CYP1B1 mRNA expression and attenuates B[*a*]P-dependent apoptosis in human PBMCs. Primary human PBMCs were transfected with an anti-miR-132 or an anti-miR control (anti-miR-CTR) (A, B, D, E) prior to a B[*a*]P-treatment for 48 h (A, B, D, E) or with the vehicle (DMSO) or 2 µM B[*a*]P for various increasing times (C). (A) Apoptosis was identified by microscopic observation of the number of cells with condensed and/or fragmented chromatin after nuclear by Hoechst 33342 staining. Data are expressed as percentages of dead cells and are shown as mean ± SEM of 6 independent experiments performed with PBMCs from separate blood donors. (B, C, D, E) mRNA expression (B, C, D, E) and miR-132 expression (C) was measured by RT-qPCR. Data are expressed relative to expression levels in DMSO-treated PBMCs, arbitrarily set at 1 unit and are shown as mean ± SEM of 6 independent experiments performed with PBMCs from separate blood donors tested in triplicate *per* experiment. *, $p \leq 0.05$ when compared with B[*a*]P-transfected PBMCs with an anti-miR-CTR (paired Student's *t* test (A, D)).

584 **References**

585 Abdullah, A., Maged, M., Hairul-Islam M, I., Osama I, A., Maha, H., Manal, A., & Hamza, H.
586 (2019). Activation of aryl hydrocarbon receptor signaling by a novel agonist ameliorates
587 autoimmune encephalomyelitis. *PloS One*, *14*(4), e0215981.
588 https://doi.org/10.1371/journal.pone.0215981

589 Bardou, P., Mariette, J., Escudié, F., Djemiel, C., & Klopp, C. (2014). jvenn: An interactive
590 Venn diagram viewer. *BMC Bioinformatics*, *15*(1), 293. https://doi.org/10.1186/1471-2105-15-
591 293

592 Bartel, D. P. (2009). MicroRNAs: Target recognition and regulatory functions. *Cell*, *136*(2),
593 215–233. https://doi.org/10.1016/j.cell.2009.01.002

594 Beer, L., Seemann, R., Ristl, R., Ellinger, A., Kasiri, M. M., Mitterbauer, A., Zimmermann, M.,
595 Gabriel, C., Gyöngyösi, M., Klepetko, W., Mildner, M., & Ankersmit, H. J. (2014). High dose
596 ionizing radiation regulates micro RNA and gene expression changes in human peripheral blood
597 mononuclear cells. *BMC Genomics*, *15*(1), 814. https://doi.org/10.1186/1471-2164-15-814

598 Boonen, I., Van Heyst, A., Van Langenhove, K., Van Hoeck, E., Mertens, B., Denison, M. S.,
599 Elskens, M., & Demaegdt, H. (2020). Assessing the receptor-mediated activity of PAHs using
600 AhR-, ERα- and PPARγ- CALUX bioassays. *Food and Chemical Toxicology: An International*
601 *Journal Published for the British Industrial Biological Research Association*, *145*, 111602.
602 https://doi.org/10.1016/j.fct.2020.111602

603 Bourgart, E., Persoons, R., Marques, M., Rivier, A., Balducci, F., von Koschembahr, A., Béal,
604 D., Leccia, M.-T., Douki, T., & Maitre, A. (2019). Influence of exposure dose, complex
605 mixture, and ultraviolet radiation on skin absorption and bioactivation of polycyclic aromatic
606 hydrocarbons ex vivo. *Archives of Toxicology*, *93*(8), 2165–2184.
607 https://doi.org/10.1007/s00204-019-02504-8

608 Chettimada, S., Lorenz, D. R., Misra, V., Wolinsky, S. M., & Gabuzda, D. (2020). Small RNA
609 sequencing of extracellular vesicles identifies circulating miRNAs related to inflammation and
610 oxidative stress in HIV patients. *BMC Immunology*, *21*(1), 57. https://doi.org/10.1186/s12865-
611 020-00386-5

612 De Flora, S., Balansky, R., D'Agostini, F., Cartiglia, C., Longobardi, M., Steele, V. E., &
613 Izzotti, A. (2012). Smoke-induced microRNA and related proteome alterations. Modulation by
614 chemopreventive agents. *International Journal of Cancer*, *131*(12), 2763–2773.
615 https://doi.org/10.1002/ijc.27814

616 Deng, Q., Dai, X., Feng, W., Huang, S., Yuan, Y., Xiao, Y., Zhang, Z., Deng, N., Deng, H.,
617 Zhang, X., Kuang, D., Li, X., Zhang, W., Zhang, X., Guo, H., & Wu, T. (2019). Co-exposure
618 to metals and polycyclic aromatic hydrocarbons, microRNA expression, and early health
619 damage in coke oven workers. *Environment International*, *122*, 369–380.
620 https://doi.org/10.1016/j.envint.2018.11.056

621 Deng, Q., Huang, S., Zhang, X., Zhang, W., Feng, J., Wang, T., Hu, D., Guan, L., Li, J., Dai,
622 X., Deng, H., Zhang, X., & Wu, T. (2014). Plasma microRNA expression and micronuclei
623 frequency in workers exposed to polycyclic aromatic hydrocarbons. *Environmental Health*
624 *Perspectives*, *122*(7), 719–725. https://doi.org/10.1289/ehp.1307080

Donate, P. B., de Lima, K. A., Peres, R. S., Almeida, F., Fukada, S. Y., Silva, T. A., Nascimento, D. C., Cecilio, N. T., Talbot, J., Oliveira, R. D., Passos, G. A., Alves-Filho, J. C., Cunha, T. M., Louzada-Junior, P., Liew, F. Y., & Cunha, F. Q. (2021). *Cigarette smoke induces miR-132 in Th17 cells that enhance osteoclastogenesis in inflammatory arthritis*. 8.

Fearnhead, H. O., Dinsdale, D., & Cohen, G. M. (1995). An interleukin-1 beta-converting enzyme-like protease is a common mediator of apoptosis in thymocytes. *FEBS Letters*, *375*(3), 283–288. https://doi.org/10.1016/0014-5793(95)01228-7

Flynt, A. S., & Lai, E. C. (2008). Biological principles of microRNA-mediated regulation: Shared themes amid diversity. *Nature Reviews. Genetics*, *9*(11), 831–842. https://doi.org/10.1038/nrg2455

Fujii-Kuriyama, Y., & Mimura, J. (2005). Molecular mechanisms of AhR functions in the regulation of cytochrome P450 genes. *Biochemical and Biophysical Research Communications*, *338*(1), 311–317. https://doi.org/10.1016/j.bbrc.2005.08.162

Gulyaeva, L. F., & Kushlinskiy, N. E. (2016). Regulatory mechanisms of microRNA expression. *Journal of Translational Medicine*, *14*(1), 143. https://doi.org/10.1186/s12967-016-0893-x

Halappanavar, S., Wu, D., Williams, A., Kuo, B., Godschalk, R. W., Van Schooten, F. J., & Yauk, C. L. (2011). Pulmonary gene and microRNA expression changes in mice exposed to benzo(a)pyrene by oral gavage. *Toxicology*, *285*(3), 133–141. https://doi.org/10.1016/j.tox.2011.04.011

Hanieh, H. (2015). Aryl hydrocarbon receptor-microRNA-212/132 axis in human breast cancer suppresses metastasis by targeting SOX4. *Molecular Cancer*, *14*, 172. https://doi.org/10.1186/s12943-015-0443-9

Hanieh, H., & Alzahrani, A. (2013). MicroRNA-132 suppresses autoimmune encephalomyelitis by inducing cholinergic anti-inflammation: A new Ahr-based exploration. *European Journal of Immunology*, *43*(10), 2771–2782. https://doi.org/10.1002/eji.201343486

Hardonnière, K., Huc, L., Sergent, O., Holme, J. A., & Lagadic-Gossmann, D. (2017). Environmental carcinogenesis and pH homeostasis: Not only a matter of dysregulated metabolism. *Seminars in Cancer Biology*, *43*, 49–65. https://doi.org/10.1016/j.semcancer.2017.01.001

Hockley, S. L., Arlt, V. M., Brewer, D., Giddings, I., & Phillips, D. H. (2006). Time- and concentration-dependent changes in gene expression induced by benzo(a)pyrene in two human cell lines, MCF-7 and HepG2. *BMC Genomics*, *7*, 260. https://doi.org/10.1186/1471-2164-7-260

Holme, J. A., Brinchmann, B. C., Refsnes, M., Låg, M., & Øvrevik, J. (2019). Potential role of polycyclic aromatic hydrocarbons as mediators of cardiovascular effects from combustion particles. *Environmental Health*, *18*, 74. https://doi.org/10.1186/s12940-019-0514-2

Hu, W.-P., Chen, Y.-C., & Chen, W.-Y. (2020). Improve sample preparation process for miRNA isolation from the culture cells by using silica fiber membrane. *Scientific Reports*, *10*, 21132. https://doi.org/10.1038/s41598-020-78202-8

Huc, L., Tekpli, X., Holme, J. A., Rissel, M., Solhaug, A., Gardyn, C., Le Moigne, G., Gorria, M., Dimanche-Boitrel, M.-T., & Lagadic-Gossmann, D. (2007). C-Jun NH2-Terminal Kinase–Related Na+/H+ Exchanger Isoform 1 Activation Controls Hexokinase II Expression in Benzo(*a*)Pyrene-Induced Apoptosis. *Cancer Research*, *67*(4), 1696–1705. https://doi.org/10.1158/0008-5472.CAN-06-2327

IARC Working Group on the Evaluation of Carcinogenic Risks to Humans, & International Agency for Research on Cancer (Eds.). (2010). *Some non-heterocyclic polycyclic aromatic hydrocarbons and some related occupational exposures*. IARC Press ; Distributed by World Health Organization.

Lagadic-Gossmann, D., Hardonnière, K., Mograbi, B., Sergent, O., & Huc, L. (2019). Disturbances in H+ dynamics during environmental carcinogenesis. *Biochimie*, *163*, 171–183. https://doi.org/10.1016/j.biochi.2019.06.013

Lagos, D., Pollara, G., Henderson, S., Gratrix, F., Fabani, M., Milne, R. S. B., Gotch, F., & Boshoff, C. (2010). MiR-132 regulates antiviral innate immunity through suppression of the p300 transcriptional co-activator. *Nature Cell Biology*, *12*(5), 513–519. https://doi.org/10.1038/ncb2054

Lee, J.-I., Zhang, L., Men, A. Y., Kenna, L. A., & Huang, S.-M. (2010). CYP-mediated therapeutic protein-drug interactions: Clinical findings, proposed mechanisms and regulatory implications. *Clinical Pharmacokinetics*, *49*(5), 295–310. https://doi.org/10.2165/11319980-000000000-00000

Liamin, M., Boutet-Robinet, E., Jamin, E. L., Fernier, M., Khoury, L., Kopp, B., Le Ferrec, E., Vignard, J., Audebert, M., & Sparfel, L. (2017). Benzo[a]pyrene-induced DNA damage associated with mutagenesis in primary human activated T lymphocytes. *Biochemical Pharmacology*, *137*, 113–124. https://doi.org/10.1016/j.bcp.2017.04.025

Liamin, M., Le Mentec, H., Evrard, B., Huc, L., Chalmel, F., Boutet-Robinet, E., Le Ferrec, E., & Sparfel, L. (2018). Genome-Wide Transcriptional and Functional Analysis of Human T Lymphocytes Treated with Benzo[α]pyrene. *International Journal of Molecular Sciences*, *19*(11), 3626. https://doi.org/10.3390/ijms19113626

Liu, H., Chang, J.-K., Hou, J.-Q., Zhao, Z.-H., & Zhang, L.-D. (2020). Inhibition of miR-221 influences bladder cancer cell proliferation and apoptosis. *European Review for Medical and Pharmacological Sciences*, *24*(14), 7550. https://doi.org/10.26355/eurrev_202007_22193

Mallah, M. A., Changxing, L., Mallah, M. A., Noreen, S., Liu, Y., Saeed, M., Xi, H., Ahmed, B., Feng, F., Mirjat, A. A., Wang, W., Jabar, A., Naveed, M., Li, J.-H., & Zhang, Q. (2022). Polycyclic aromatic hydrocarbon and its effects on human health: An overeview. *Chemosphere*, *296*, 133948. https://doi.org/10.1016/j.chemosphere.2022.133948

Martin-Way, D., Puche-Sanz, I., Cozar, J. M., Zafra-Gomez, A., Gomez-Regalado, M. D. C., Morales-Alvarez, C. M., Hernandez, A. F., Martinez-Gonzalez, L. J., & Alvarez-Cubero, M. J. (2022). Genetic variants of antioxidant enzymes and environmental exposures as molecular biomarkers associated with the risk and aggressiveness of bladder cancer. *The Science of the Total Environment*, *843*, 156965. https://doi.org/10.1016/j.scitotenv.2022.156965

Mayati, A., Levoin, N., Paris, H., N'Diaye, M., Courtois, A., Uriac, P., Lagadic-Gossmann, D., Fardel, O., & Le Ferrec, E. (2012). Induction of Intracellular Calcium Concentration by Environmental Benzo(a)pyrene Involves a β2-Adrenergic Receptor/Adenylyl Cyclase/Epac-1/Inositol 1,4,5-Trisphosphate Pathway in Endothelial Cells. *The Journal of Biological Chemistry*, *287*(6), 4041–4052. https://doi.org/10.1074/jbc.M111.319970

Mizushima, N., & Yoshimori, T. (2007). How to Interpret LC3 Immunoblotting. *Autophagy*, *3*(6), 542–545. https://doi.org/10.4161/auto.4600

Ogando, J., Tardáguila, M., Díaz-Alderete, A., Usategui, A., Miranda-Ramos, V., Martínez-Herrera, D. J., de la Fuente, L., García-León, M. J., Moreno, M. C., Escudero, S., Cañete, J. D., Toribio, M. L., Cases, I., Pascual-Montano, A., Pablos, J. L., & Mañes, S. (2016). Notch-regulated miR-223 targets the aryl hydrocarbon receptor pathway and increases cytokine production in macrophages from rheumatoid arthritis patients. *Scientific Reports*, *6*, 20223. https://doi.org/10.1038/srep20223

Prieto-Fernández, E., Aransay, A. M., Royo, F., González, E., Lozano, J. J., Santos-Zorrozua, B., Macias-Camara, N., González, M., Garay, R. P., Benito, J., Garcia-Orad, A., & Falcón-Pérez, J. M. (2019). A Comprehensive Study of Vesicular and Non-Vesicular miRNAs from a Volume of Cerebrospinal Fluid Compatible with Clinical Practice. *Theranostics*, *9*(16), 4567–4579. https://doi.org/10.7150/thno.31502

Prigent, L., Robineau, M., Jouneau, S., Morzadec, C., Louarn, L., Vernhet, L., Fardel, O., & Sparfel, L. (2014). The aryl hydrocarbon receptor is functionally upregulated early in the course of human T-cell activation: Cellular immune response. *European Journal of Immunology*, *44*(5), 1330–1340. https://doi.org/10.1002/eji.201343920

Rani, R. (2021). Circulating microRNAs as biomarkers of environmental exposure to polycyclic aromatic hydrocarbons: Potential and prospects. *Environ Sci Pollut Res*, 17.

Rieger, J. K., Klein, K., Winter, S., & Zanger, U. M. (2013). Expression variability of absorption, distribution, metabolism, excretion-related microRNAs in human liver: Influence of nongenetic factors and association with gene expression. *Drug Metabolism and Disposition: The Biological Fate of Chemicals*, *41*(10), 1752–1762. https://doi.org/10.1124/dmd.113.052126

Ruiz-Vera, T., Ochoa-Martínez, Á. C., Pruneda-Álvarez, L. G., Domínguez-Cortinas, G., & Pérez-Maldonado, I. N. (2019). Expression levels of circulating microRNAs-126, -155, and -145 in Mexican women exposed to polycyclic aromatic hydrocarbons through biomass fuel use: Expression Levels of Circulating MicroRNAs-126, -155, and -145 in Mexican Women Exposed to Polycyclic Aromatic Hydrocarbons through Biomass Fuel Use. *Environmental and Molecular Mutagenesis*. https://doi.org/10.1002/em.22273

Sağır, F., Ersoy Tunalı, N., Tombul, T., Koral, G., Çırak, S., Yılmaz, V., Türkoğlu, R., & Tüzün, E. (2021). miR-132-3p, miR-106b-5p, and miR-19b-3p Are Associated with Brain-Derived Neurotrophic Factor Production and Clinical Activity in Multiple Sclerosis: A Pilot Study. *Genetic Testing and Molecular Biomarkers*, *25*(11), 720–726. https://doi.org/10.1089/gtmb.2021.0183

Shimada, T. (2006). Xenobiotic-metabolizing enzymes involved in activation and detoxification of carcinogenic polycyclic aromatic hydrocarbons. *Drug Metabolism and Pharmacokinetics*, *21*(4), 257–276. https://doi.org/10.2133/dmpk.21.257

Sparfel, L., Pinel-Marie, M.-L., Boize, M., Koscielny, S., Desmots, S., Pery, A., & Fardel, O. (2010). Transcriptional signature of human macrophages exposed to the environmental contaminant benzo(a)pyrene. *Toxicological Sciences: An Official Journal of the Society of Toxicology*, *114*(2), 247–259. https://doi.org/10.1093/toxsci/kfq007

Sparfel, L., Van Grevenynghe, J., Le Vee, M., Aninat, C., & Fardel, O. (2006). Potent inhibition of carcinogen-bioactivating cytochrome P450 1B1 by the p53 inhibitor pifithrin α. *Carcinogenesis*, *27*(3), 656–663. https://doi.org/10.1093/carcin/bgi256

Stading, R., Gastelum, G., Chu, C., Jiang, W., & Moorthy, B. (2021). Molecular mechanisms of pulmonary carcinogenesis by polycyclic aromatic hydrocarbons (PAHs): Implications for human lung cancer. *Seminars in Cancer Biology*, *76*, 3–16. https://doi.org/10.1016/j.semcancer.2021.07.001

Thomé, M. P., Filippi-Chiela, E. C., Villodre, E. S., Migliavaca, C. B., Onzi, G. R., Felipe, K. B., & Lenz, G. (2016). Ratiometric analysis of Acridine Orange staining in the study of acidic organelles and autophagy. *Journal of Cell Science*, *129*(24), 4622–4632. https://doi.org/10.1242/jcs.195057

Tumolo, M. R., Panico, A., De Donno, A., Mincarone, P., Leo, C. G., Guarino, R., Bagordo, F., Serio, F., Idolo, A., Grassi, T., & Sabina, S. (2022). The expression of microRNAs and exposure to environmental contaminants related to human health: A review. *International Journal of Environmental Health Research*, *32*(2), 332–354. https://doi.org/10.1080/09603123.2020.1757043

Uno, S., Dalton, T. P., Dragin, N., Curran, C. P., Derkenne, S., Miller, M. L., Shertzer, H. G., Gonzalez, F. J., & Nebert, D. W. (2006). Oral benzo[a]pyrene in Cyp1 knockout mouse lines: CYP1A1 important in detoxication, CYP1B1 metabolism required for immune damage independent of total-body burden and clearance rate. *Molecular Pharmacology*, *69*(4), 1103–1114. https://doi.org/10.1124/mol.105.021501

van Grevenynghe, J., Sparfel, L., Le Vee, M., Gilot, D., Drenou, B., Fauchet, R., & Fardel, O. (2004). Cytochrome P450-dependent toxicity of environmental polycyclic aromatic hydrocarbons towards human macrophages. *Biochemical and Biophysical Research Communications*, *317*(3), 708–716. https://doi.org/10.1016/j.bbrc.2004.03.104

van Meteren, N., Lagadic-Gossmann, D., Chevanne, M., Gallais, I., Gobart, D., Burel, A., Bucher, S., Grova, N., Fromenty, B., Appenzeller, B. M. R., Chevance, S., Gauffre, F., Le Ferrec, E., & Sergent, O. (2019). Polycyclic Aromatic Hydrocarbons Can Trigger Hepatocyte Release of Extracellular Vesicles by Various Mechanisms of Action Depending on Their Affinity for the Aryl Hydrocarbon Receptor. *Toxicological Sciences*, *171*(2), 443–462. https://doi.org/10.1093/toxsci/kfz157

van Meteren, N., Lagadic-Gossmann, D., Podechard, N., Gobart, D., Gallais, I., Chevanne, M., Collin, A., Dupont, A., & Rault, L. (2020). *Extracellular vesicles released by polycyclic aromatic hydrocarbons-treated hepatocytes trigger oxidative stress in recipient hepatocytes by delivering iron*. 59.

Vrijens, K., Bollati, V., & Nawrot, T. S. (2015). MicroRNAs as Potential Signatures of Environmental Exposure or Effect: A Systematic Review. *Environmental Health Perspectives*, *123*(5), 399–411. https://doi.org/10.1289/ehp.1408459

Wanet, A., Tacheny, A., Arnould, T., & Renard, P. (2012). miR-212/132 expression and functions: Within and beyond the neuronal compartment. *Nucleic Acids Research*, *40*(11), 4742–4753. https://doi.org/10.1093/nar/gks151

Wu, B., Li, J., Wang, H., Wu, Q., & Liu, H. (2020). MiR-132-3p serves as a tumor suppressor in mantle cell lymphoma via directly targeting SOX11. *Naunyn-Schmiedeberg's Archives of Pharmacology*, *393*(11), 2197–2208. https://doi.org/10.1007/s00210-020-01834-0

Wu, M., Liang, G., Duan, H., Yang, X., Qin, G., & Sang, N. (2019). Synergistic effects of sulfur dioxide and polycyclic aromatic hydrocarbons on pulmonary pro-fibrosis via mir-30c-1-3p/ transforming growth factor β type II receptor axis. *Chemosphere*, *219*, 268–276. https://doi.org/10.1016/j.chemosphere.2018.12.016

Xie, M.-Y., Chen, T., Xi, Q.-Y., Hou, L.-J., Luo, J.-Y., Zeng, B., Li, M., Sun, J.-J., & Zhang, Y.-L. (2020). Porcine milk exosome miRNAs protect intestinal epithelial cells against deoxynivalenol-induced damage. *Biochemical Pharmacology*, *175*, 113898. https://doi.org/10.1016/j.bcp.2020.113898

Yagi, Y., Ohkubo, T., Kawaji, H., Machida, A., Miyata, H., Goda, S., Roy, S., Hayashizaki, Y., Suzuki, H., & Yokota, T. (2017). Next-generation sequencing-based small RNA profiling of cerebrospinal fluid exosomes. *Neuroscience Letters*, *636*, 48–57. https://doi.org/10.1016/j.neulet.2016.10.042

Yu, Y., Jin, H., & Lu, Q. (2022). Effect of polycyclic aromatic hydrocarbons on immunity. *Journal of Translational Autoimmunity*, *5*, 100177. https://doi.org/10.1016/j.jtauto.2022.100177

Zhao, B., DeGroot, D. E., Hayashi, A., He, G., & Denison, M. S. (2010). CH223191 Is a Ligand-Selective Antagonist of the Ah (Dioxin) Receptor. *Toxicological Sciences*, *117*(2), 393–403. https://doi.org/10.1093/toxsci/kfq217

824

Table 1: Top functions regulated by the 15 differentially-expressed miRNAs in PBMCs after exposure to 2 µM B[*a*]P for 48 h.

Molecular and Cellular functions		
Top Functions	***p-value*[a]**	**miRNAs**
Cellular Development	3.98E-02 - 4.83E-06	130a-3p, 132-3p, 144-5p, 221-3p, 23a-3p, 30c-5p, 320b, 7a-5p
Cellular Growth and Proliferation	3.98E-02 - 4.83E-06	130a-3p, 132-3p, 144-5p, 221-3p, 23a-3p, 30c-5p, 320b, 7a-5p
Cell Death and Survival	4.87E-02 - 1.96E-04	130a-3p, 132-3p, 142-3p, 221-3p, 23a-3p, 30c-5p, 320b, 7a-5p
Cell-To-Cell Signaling and Interaction	3.32E-02 - 1.38E-03	142-3p, 221-3p
Cellular Function and Maintenance	4.16E-02 - 1.84E-03	130a-3p, 142-3p, 30c-5p, 320b

[a]p-values were calculated using the IPA software.

825

A

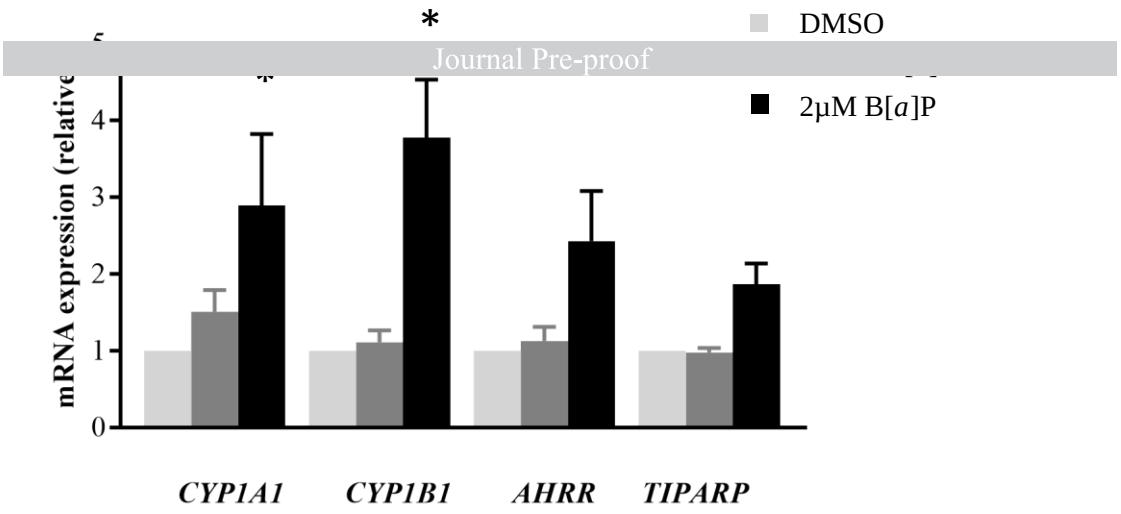

B

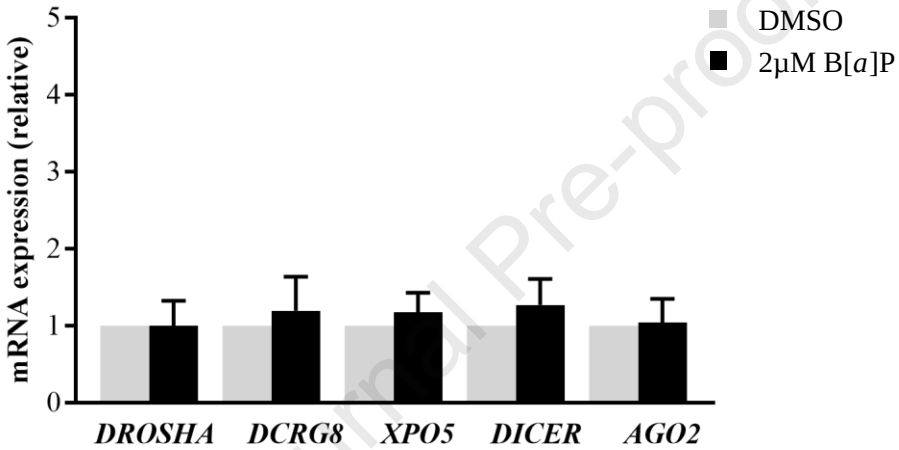

C

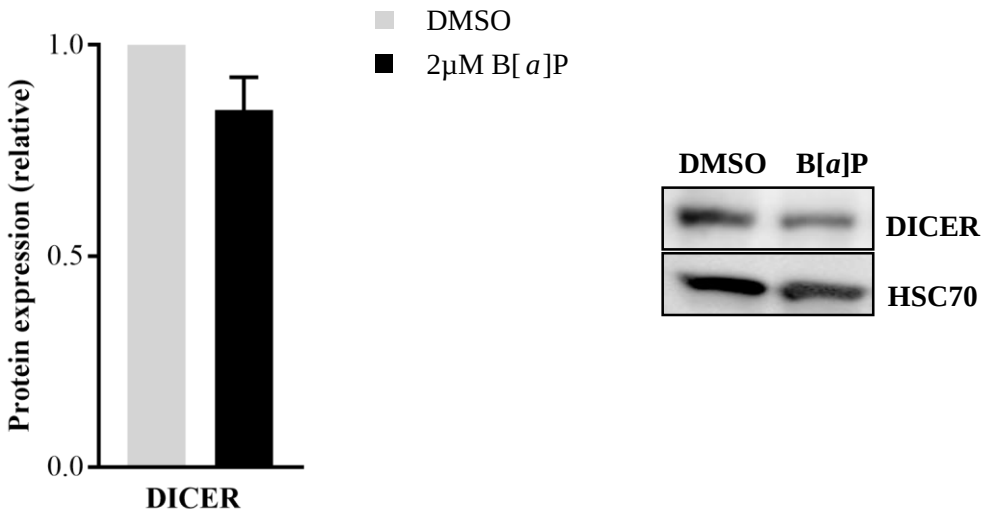

Fig. 1

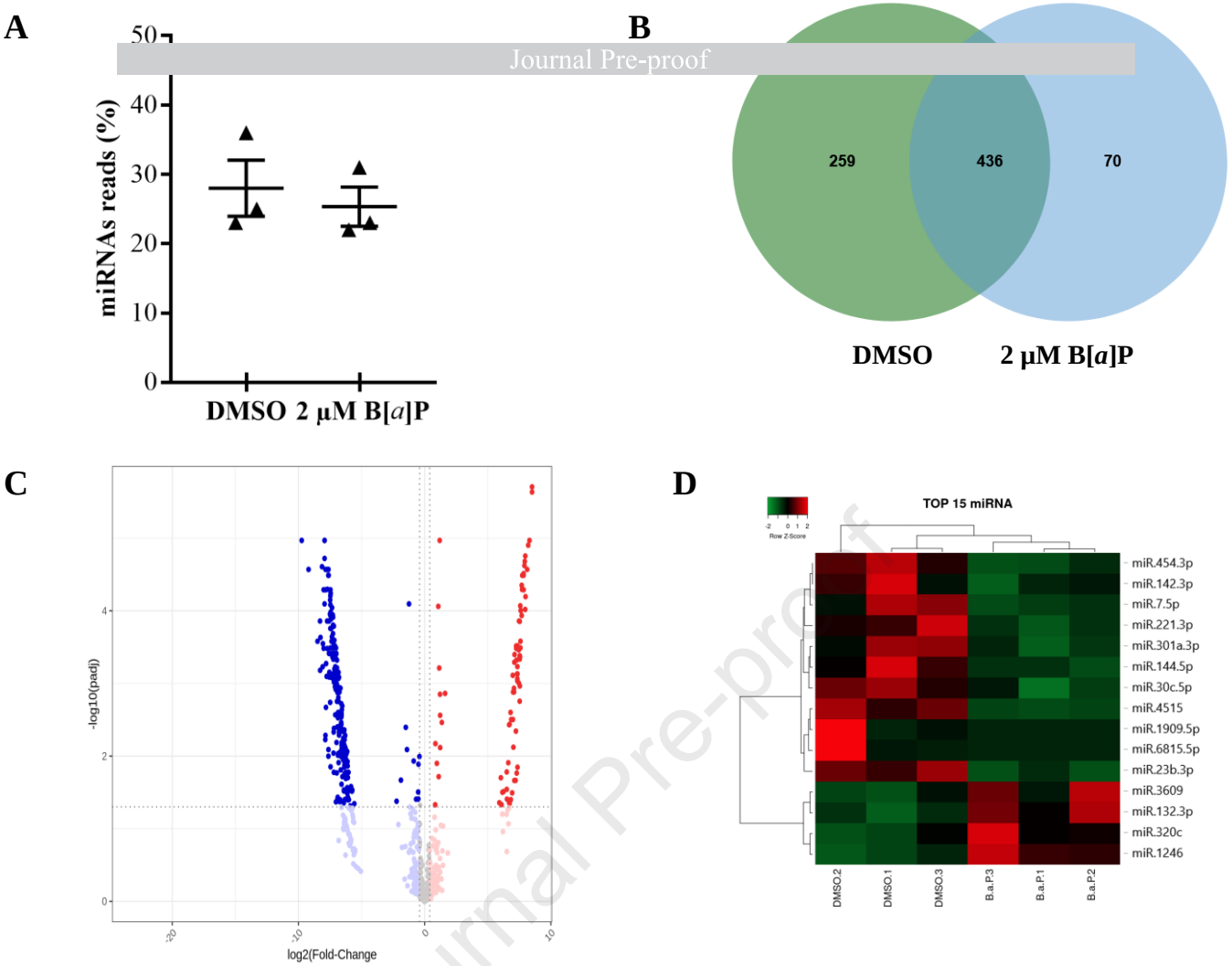

E

	baseMean	log2FoldChange	*p-value*	*p-value* adjusted
hsa-miR-142-3p	48920.68	-0.7	0.01	0.04
hsa-miR-221-3p	7113.01	-0.4	0.02	0.05
hsa-miR-23b-3p	3104.84	-0.4	0.00	0.01
hsa-miR-1246	1708.11	1.2	0.00	0.00
hsa-miR-132-3p	934.27	1.2	0.00	0.00
hsa-miR-454-3p	1536.52	-0.5	0.00	0.01
hsa-miR-30c-5p	1467.31	-0.5	0.01	0.03
hsa-miR-320c	809.59	0.8	0.02	0.05
hsa-miR-7-5p	1121.42	-0.5	0.01	0.04
hsa-miR-3609	412.29	1.1	0.01	0.02
hsa-miR-144-5p	372.74	-0.9	0.00	0.01
hsa-miR-4515	254.03	-1.2	0.00	0.00
hsa-miR-301a-3p	115.06	-1.0	0.02	0.05
hsa-miR-1909-5p	85.36	-9.7	0.00	0.00
hsa-miR-6815-5p	58.60	-9.2	0.00	0.00

Fig. 2

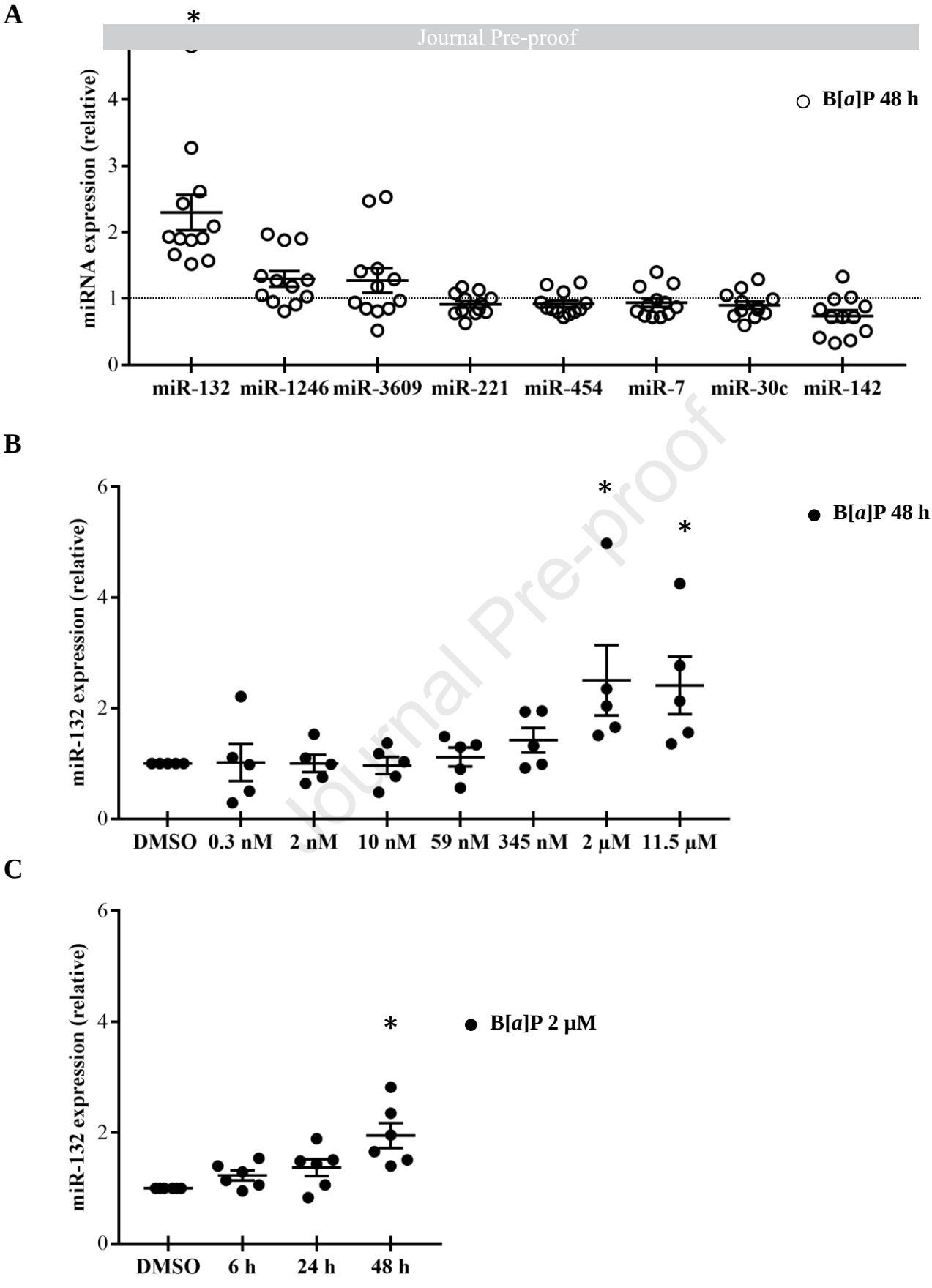

Fig. 3

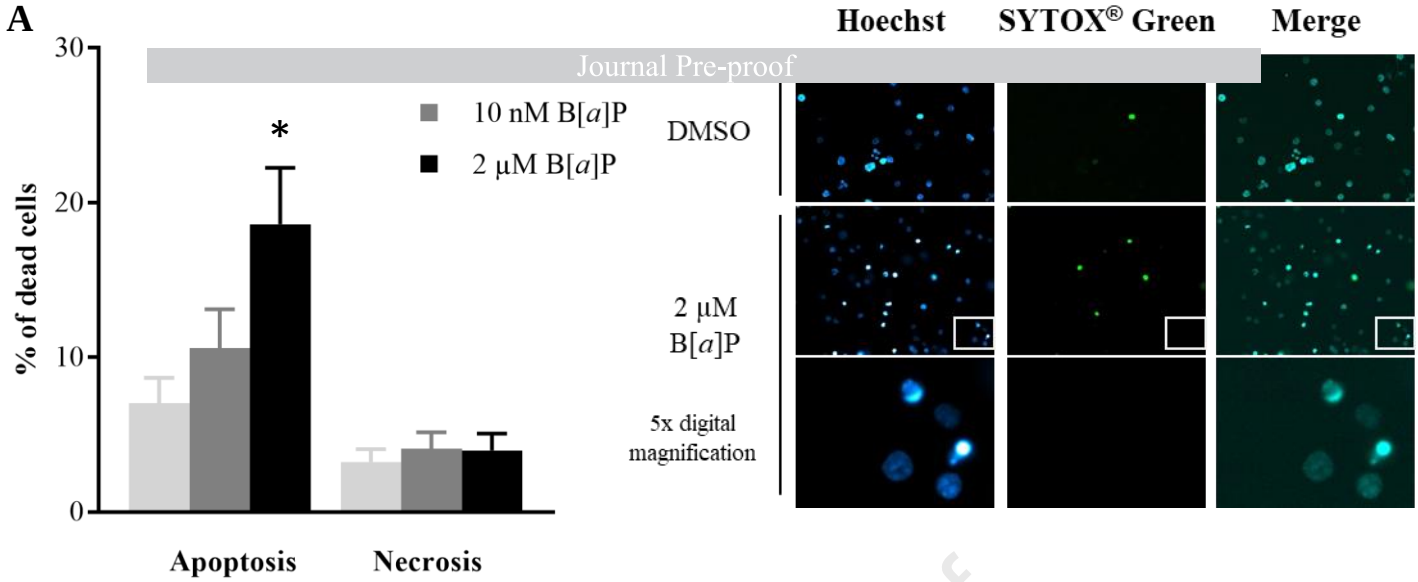

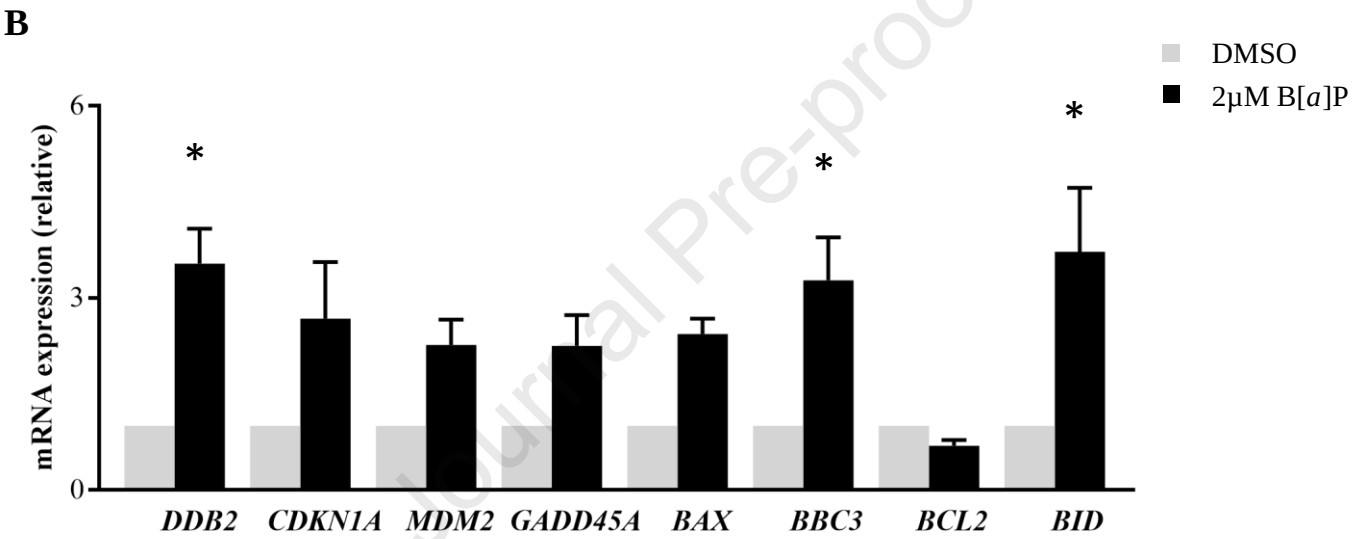

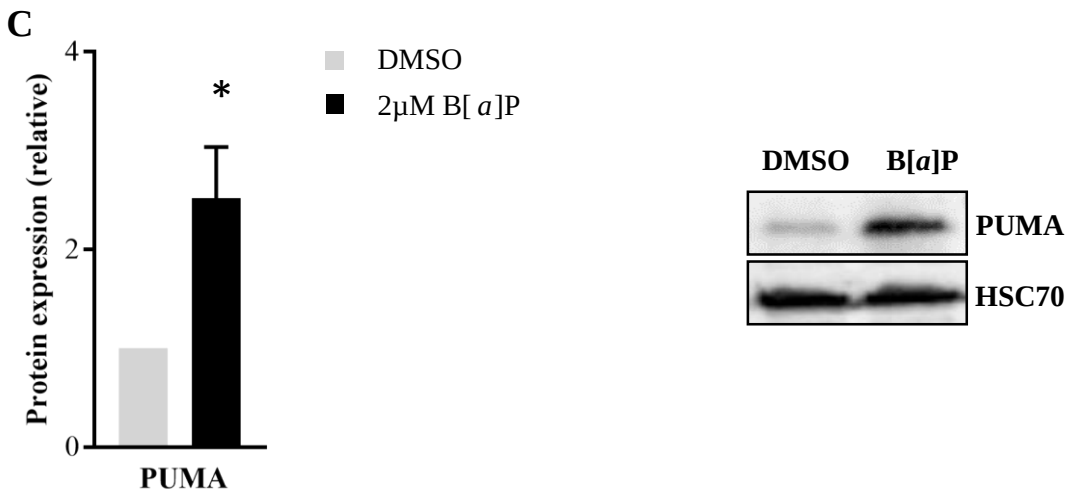

Fig. 4

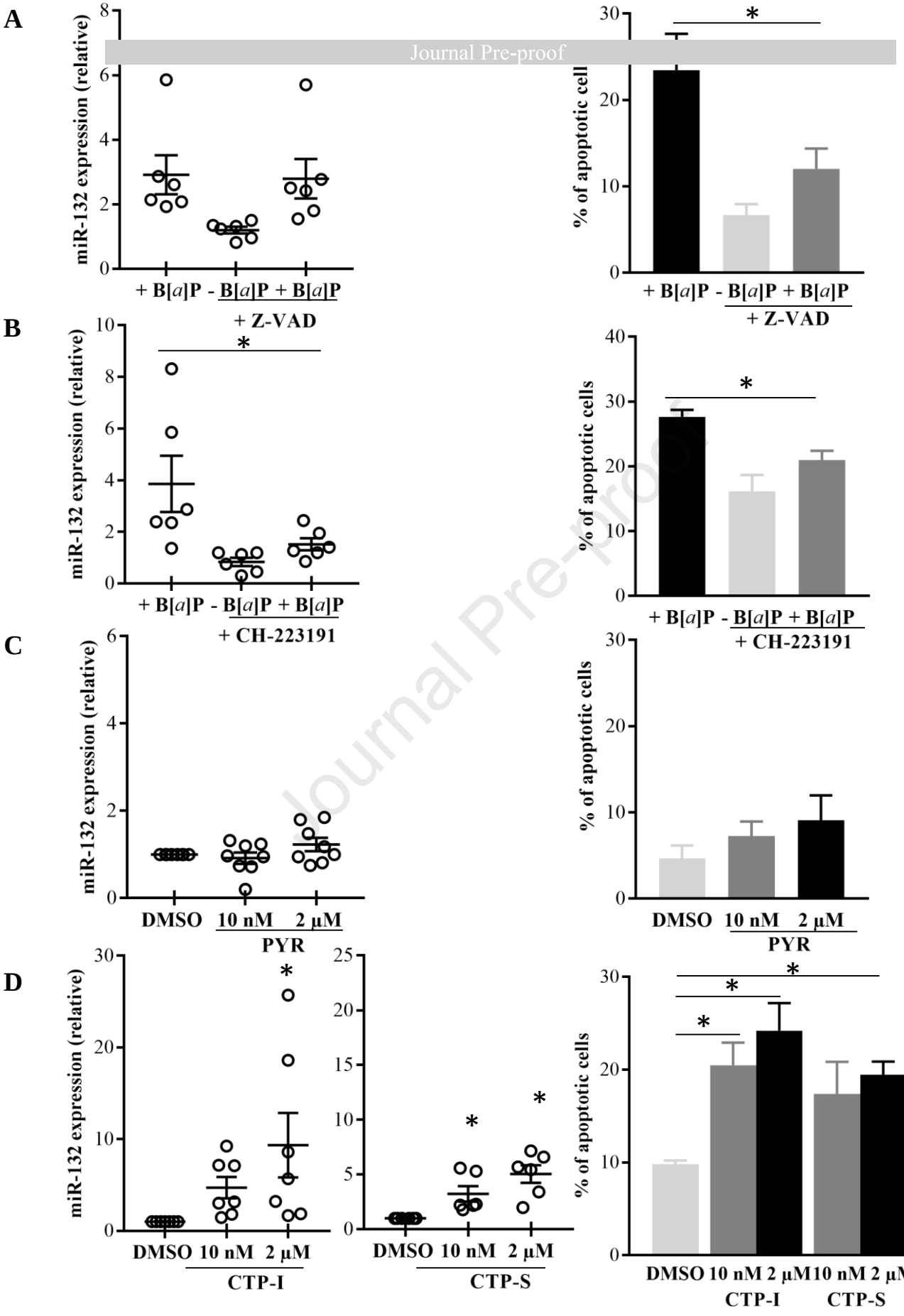

Fig. 5

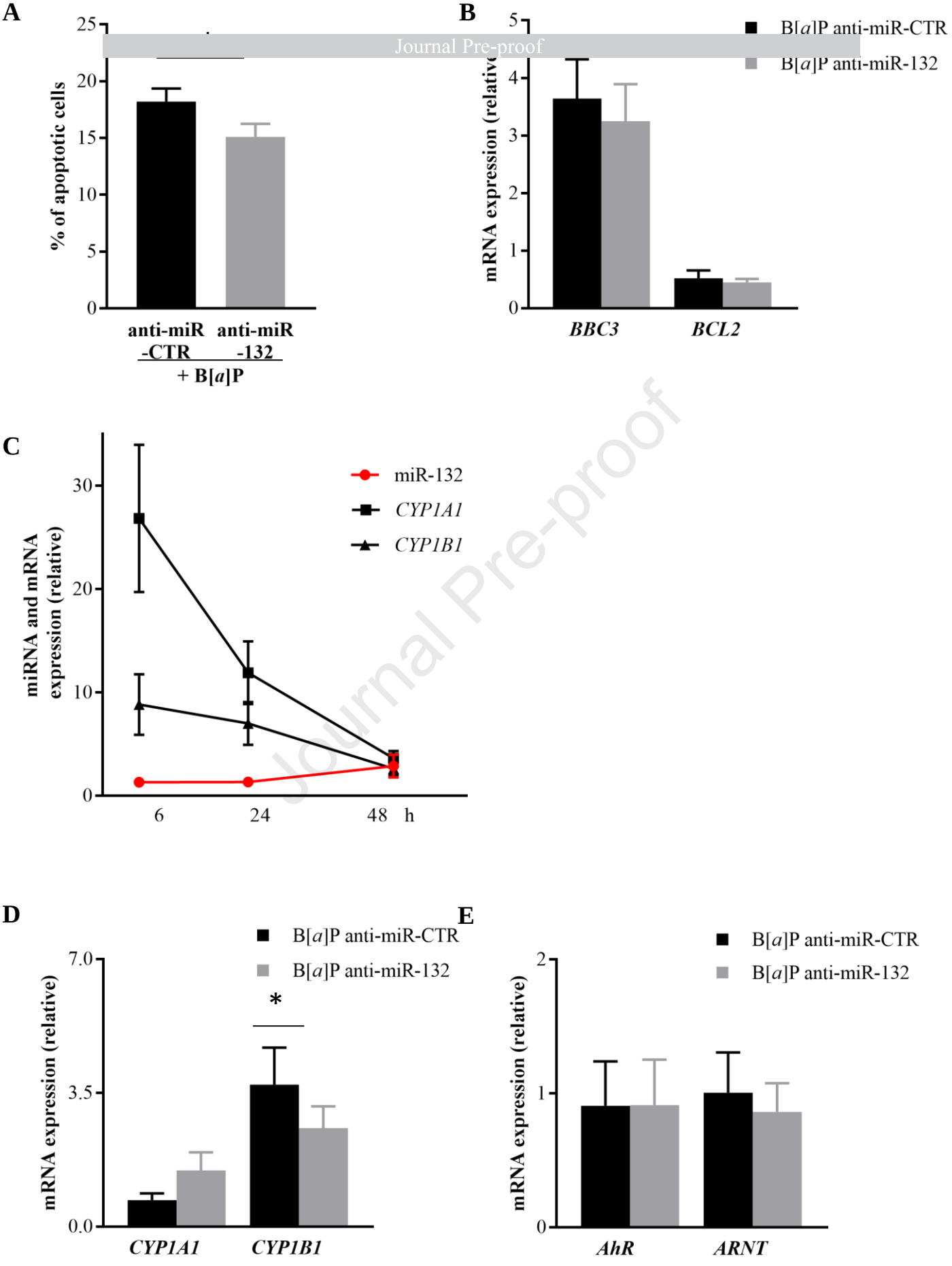

Fig. 6

Highlights

- Small RNA sequencing identifies B[*a*]P-responsive miRNAs in human PBMCs.
- Predicted targets of B[*a*]P-regulated miRNAs are related to apoptosis of PBMCs.
- miR-132-3p is the most B[*a*]P-regulated miRNA in PBMCs.
- B[*a*]P-induced miR-132 requires AhR activation.
- miR-132 could modulate apoptosis *via* regulation of the CYP1A1/1B1 balance upon B[*a*]P.

Author Contributions

Conceptualization: Dominique Lagadic-Gossmann, Normand Podechard and Lydie Sparfel

Methodology: Rima Souki, Jérémy Amossé, Valentine Genêt, Franck Letourneur, Dominique Lagadic-Gossmann, Normand Podechard and Lydie Sparfel

Software: Morgane Le Gall, Benjamin SaintPierre, Franck Letourneur and Lydie Sparfel

Validation: Rima Souki, Jérémy Amossé, Valentine Genêt, Franck Letourneur, Normand Podechard

Formal analysis: Rima Souki, Jérémy Amossé, Valentine Genêt, Morgane Le Gall, Benjamin SaintPierre and Lydie Sparfel

Investigation: Rima Souki, Jérémy Amossé, Valentine Genêt, Eric Le Ferrec, Dominique Lagadic-Gossmann, Normand Podechard and Lydie Sparfel

Resources : Morgane Le Gall, Benjamin SaintPierre, Anne Maître, Christine Demeilliers

Data curation: Benjamin SaintPierre and Lydie Sparfel

Writing – original draft: Lydie Sparfel

Writing – review & editing: Rima Souki, Jérémy Amossé, Valentine Genêt, Morgane Le Gall, Benjamin SaintPierre, Franck Letourneur, Anne Maître, Christine Demeilliers, Eric Le Ferrec, Dominique Lagadic-Gossmann, Normand Podechard and Lydie Sparfel

Visualization: Rima Souki, Jérémy Amossé, Valentine Genêt, Morgane Le Gall, Benjamin SaintPierre and Lydie Sparfel

Supervision: Lydie Sparfel

Project administration: Lydie Sparfel

Funding acquisition: Lydie Sparfel

Declaration of interests

☒ The authors declare that they have no known competing financial interests or personal relationships that could have appeared to influence the work reported in this paper.

☐ The authors declare the following financial interests/personal relationships which may be considered as potential competing interests: